Biomaterials 35 (2014) 1857–1868

Contents lists available at ScienceDirect

Biomaterials

journal homepage: www.elsevier.com/locate/biomaterials

The effect of time-dependent deformation of viscoelastic hydrogels on myogenic induction and Rac1 activity in mesenchymal stem cells

Andrew R. Cameron [a], Jessica E. Frith [a], Guillermo A. Gomez [b], Alpha S. Yap [b], Justin J. Cooper-White [a,c,d,*]

[a] Tissue Engineering and Microfluidics Laboratory, The Australian Institute for Bioengineering and Nanotechnology, University of Queensland, St Lucia, QLD, Australia
[b] Division of Molecular Cell Biology, Institute for Molecular Bioscience, University of Queensland, St Lucia, QLD, Australia
[c] School of Chemical Engineering, University of Queensland, St Lucia, QLD, Australia
[d] CSIRO, Division of Materials Science and Engineering, Clayton, Victoria, Australia

ARTICLE INFO

Article history:
Received 14 October 2013
Accepted 7 November 2013
Available online 9 December 2013

Keywords:
Mesenchymal stem cell
Smooth muscle cell
Creep
Viscoelasticity
Hydrogel
Mechanotransduction

ABSTRACT

Cell behaviours within tissues are influenced by a broad array of physical and biochemical microenvironmental factors. Whilst 'stiffness' is a recognised physical property of substrates and tissue microenvironments that influences many cellular behaviours, tissues and their extracellular matrices are not purely rigid but 'viscoelastic' materials, composed of both rigid-like (elastic) and dissipative (viscous) elements. This viscoelasticity results in materials displaying increased deformation with time under the imposition of a defined force or stress, a phenomenon referred to as time-dependent deformation or 'creep'. Previously, we compared the behaviour of human mesenchymal stem cells (hMSCs) on hydrogels tailored to have a constant stiffness, but to display varying levels of creep in response to an applied force. Using polyacrylamide as a model material, we showed that on high-creep hydrogels (HCHs), hMSCs displayed increased proliferation, spread area and differentiation towards multiple lineages, compared to their purely stiff analogue, with a particular propensity for differentiation towards a smooth muscle cell (SMC) lineage. In this present study, we investigate the mechanisms behind this phenomenon and show that hMSCs adhered to HCHs have increased expression of SMC induction factors, including soluble factors, ECM proteins and the cell–cell adhesion molecule, N-Cadherin. Further, we identify a key role for Rac1 signalling in mediating this increased N-Cadherin expression. Using a real-time Rac1-FRET biosensor, we confirm increased Rac1 activation on HCHs, an observation that is further supported functionally by observed increases in motility and lamellipodial protrusion rates of hMSCs. Increased Rac1 activity in hMSCs on HCHs provides underlying mechanisms for enhanced commitment towards a SMC lineage and the compensatory increase in spread area (isotonic tension) after a creep-induced loss of cytoskeletal tension on viscoelastic substrates, in contrast to previous studies that have consistently demonstrated up-regulation of RhoA activity with increasing substrate stiffness. Tuning substrate viscoelasticity to introduce varying levels of creep thus equips the biomaterial scientist or engineer with a new tool with which to tune and direct stem cell outcomes.

1. Introduction

The intrinsic behaviours of cells, *in vitro* and *in vivo*, are significantly affected by the physical and biochemical microenvironment in which they reside [1,2]. This is especially true for cells having significant plasticity, such as mesenchymal stem cells (MSCs) [3–8]. It has emerged most recently that mechanical cues, derived from various modes of stimulation, can play an important role in influencing the differentiation of MSCs into various tissue cell endpoints, including muscle [3,4]. Externally applied mechanical stimulation of a matrix (through stretching or compression of the matrix) has been shown to induce or up-regulate secretion of cytokines, such as TGF-β_1 [9,10], and ECM molecules, such as laminin [11], in adhered cells, both of which were shown to drive smooth muscle cell (SMC) differentiation of hMSCs [12–16]. In the case of pluripotent stem cells, this was shown to be through autocrine actions [17,18]. However, in

* Corresponding author. Tissue Engineering and Microfluidics Laboratory, Australian Institute for Bioengineering and Nanotechnology, The University of Queensland, St. Lucia, Queensland 4072, Australia. Tel.: +61 7 3346 3858.
E-mail address: j.cooperwhite@uq.edu.au (J.J. Cooper-White).

0142-9612/$ – see front matter
http://dx.doi.org/10.1016/j.biomaterials.2013.11.023

the absence of such external mechanical stimulation, cells themselves also apply force locally to a matrix through their adhesions. In deforming the surrounding matrix, cells experience a resistive force, the magnitude and time scales of which are defined by the intrinsic mechanical properties of the matrix. This substrate-induced mechanical feedback is also capable of driving cellular behaviours – for example, the stiffness (or compressive modulus) of a substrate, which represents just one mechanical property of a material, has been shown to direct multiple fate choices of hMSCs, including lineage commitment to muscle cells [3].

Most tissues, and indeed many synthetic biomaterials, are not purely elastic but 'viscoelastic' in nature, being composed of both elastic and viscous elements. The resulting spectrum of mechanical properties that cells may sense when attached to a matrix is thus more appropriately described not only by a 'stiffness' value, but instead by its viscoelasticity, in terms of both an elastic component, which can be represented by the storage modulus (G′), and a dissipative or viscous component, represented by the loss modulus (G″). The *higher* the magnitude of the dissipative component (G″) of a matrix, at a constant elastic component contribution (G′), the *more* time dependent deformation incurred under an applied force (such as that applied by an adhered cell), a behaviour that is referred to as 'creep'. One can thus appreciate that as adherent cells begin to exert force on a viscoelastic substrate via their focal adhesions (FAs), in contrast to a purely elastic substrate, substrate creep may result in cells feeling a time dependent reduction in the resistive force they experience when actively pulling on a substrate. This reduction in resistive force, due to the dissipative elements in viscoelastic materials, would be expected to impact not only the size and maturity of the FAs [19], but many other downstream cellular processes. Elucidating the effect of matrix creep on cell behaviour may thus have significant implications in understanding how cells interact with their native 'viscoelastic' microenvironments *in vivo*, as well as predicting how cells will respond to synthetically developed biomaterials.

Indeed, a recent investigation by our group has demonstrated that the dissipative component or loss modulus (G″) of a material's mechanical property slate can significantly influence multiple hMSC behaviours, including differentiation [20]. In stark contrast to the observed capacity of substrates of differing levels of stiffness to *bias* the differentiation of hMSCs into defined tissue endpoints [3], we showed that on a set of viscoelastic polyacrylamide (PAM) hydrogels that displayed increasing levels of creep (but a constant stiffness matched to that of muscle tissue (13.5 kPa)) [20], hMSCs not only showed enhanced differentiation towards a myogenic fate, but also towards osteo- and adipogenic fates when in the presence of inductive factors [20]. However, unlike the effect of creep on osteogenesis or adipogenesis of hMSCs, myogenesis (or more specifically SMC differentiation) was enhanced in *both* basal and myogenic differentiation medium [20]. This was demonstrated by an observed increase in expression of early- and mid-stage SMC markers, αSMC and calponin, on high creep hydrogels (HCHs) compared to low creep hydrogels (LCHs), suggesting an increased propensity for spontaneous induction of SMC differentiation of hMSCs on these hydrogels [20]. This study further confirmed that the enhanced differentiation of hMSCs on substrates of increasing creep was the result of the time dependent decrease in both *passive* and actively generated *isometric* cytoskeletal tension [20], terms previously defined by the cellular tensegrity model [21,22]. In line with this model, it was proposed that hMSCs adhered to these types of substrates would attempt to restore the balance of this lost tension through alternative mechanisms, such as increased spread area (*isotonic* cytoskeletal tension) and increased cell–cell contact (passive tension), behaviours both associated with hMSC differentiation [23,24].

These particular viscoelastic PAM hydrogels more closely mimic *in vivo* tissue mechanics than the purely elastic PAM materials previously utilised, and their use with hMSCs has already lead to new insight into the impacts of the dissipative component of a material's viscoelastic spectrum on stem cell fate choice. However, the exact molecular mechanism by which hMSCs respond to such a mechanical property during and post adhesion is currently unknown.

The current investigation thus aimed to investigate the driver/s behind the observed enhanced smooth muscle myogenesis of hMSCs when adhered to viscoelastic substrates of constant stiffness (approximating muscle tissue) but varying levels of creep. Importantly, we investigate both end point expression (at defined time points) and real time (dynamic) activation of key regulatory proteins within known mechanotransduction pathways, using a range of standard molecular biology techniques and a cellular Rac1 biosensor, exposing the critical role Rac1 (a Rho GTPase) plays in directing the observed behaviours of hMSCs on these tailored viscoelastic substrates.

2. Materials and methods

2.1. Gel fabrication

As previously described [20], PAM gels were formulated from solutions of 30 wt % *Acryl* (Sigma–Aldrich) and 1 wt% *Bis* (Sigma–Aldrich) and crosslinked using tetramethylethylenediamine (TEMED) (Bio-Rad, Regents Park, Australia) and 10 wt% ammonia persulphate (Amresco) in an oxygen free environment (under nitrogen) for approximately 30 min. Thin gels used in the FRET biosensor analysis were attached to the underlying glass by washing the glass with 0.1 M NaOH, silanising the dried surface with aminopropyltriethoxysilane (APTS) for 5 min, washing the surface thoroughly with milli-Q water and then applying 1% glutaraldehyde in PBS for 30 min. The surfaces were washed with milli-Q water and air dried.

2.2. Gel functionalisation for cell seeding

Sulfosuccinimidyl 6(4′-azido-2′-nitrophenyl-amino) hexanoate (SANPAH) (Thermo Fisher) was photocrosslinked to the surface of the gels at a concentration of 1 mg/mL using UV light for 30 min. Gels were thoroughly washed in PBS and functionalised with 50 μg/mL type I collagen (bovine derived) (Devro Medical) by soaking the SANPAH treated gels in collagen solution overnight at 4 °C. Gels were again washed with PBS before cell seeding.

2.3. Differentiation, TGF-β_1, ECM protein and N-Cad analysis

2.3.1. Cell culture conditions

hMSCs were obtained from the Mater Medical Research Institute, Brisbane and used under approval from the Medical Research Ethics Committee at the University of Queensland (#2010001069). For analysis, hMSCs were seeded at 4000 cells/cm^2 and cultured in growth or differentiation medium for 7 days before samples were collected for analysis. Growth medium (GM) consisted of low-glucose DMEM supplemented with 10% FBS and 1% penicillin/streptomycin. Myogenic medium consisted of GM supplemented with 10 ng/mL TGF-β_1 and 30 μM ascorbic acid. Osteogenic medium consisted of GM supplemented with 2 mM L-glutamine, 0.1 μM dexamethasone, 50 μM ascorbic acid, and 10 mM β-glycerophosphate. Adipogenic medium consisted of high-glucose DMEM supplemented with 10% FBS, 1% penicillin/streptomycin, 0.2 mM indomethacin, 1 μM dexamethasone, 0.5 mM IBMX, and 10 μg/mL insulin. Mixed osteogenic/adipogenic medium contained 1:1 adipogenic:osteogenic differentiation media.

2.3.2. Quantitative real-time reverse transcription polymerase chain reaction (qPCR)

2.3.2.1. RNA isolation and cDNA synthesis. Total RNA was isolated using an RNeasy Mini Kit with on-column DNase treatment (QIAGEN VWR, Stockholm, Sweeden) according to the protocol given by the manufacturer. The concentration and purity of RNA were determined by using a Nano-Drop spectrophotometer (NanoDrop Technologies, Inc., Rockland, DE). cDNA was synthesised from up to 200 ng of RNA (with equal amounts for all samples in one experiment) using SuperScript III First-Strand Synthesis SuperMix (Invitrogen) in a total volume of 21 μL, as per manufacturer's instructions. An equivalent volume of DNase and RNase-free water was used in place of RT Enzyme Mix for no-RT controls.

2.3.2.2. Quantitative real-time reverse transcription polymerase chain reaction (qPCR). qPCR reactions were set up in triplicates with each reaction having a total volume of 10 μL containing 1X Platinum SYBR Green qPCR SuperMix-UGD (Invitrogen), 0.2 μM forward and reverse primers (Table 1) and 1 μL cDNA. A 7500 Fast Real-Time PCR System (Applied Biosystems) was used at standard cycling parameters of 50 °C for 2 min, 95 °C for 2 min and then 95 °C for 15 s and 60 °C for 30 s for a total of 40

Table 1
Primer sequences used in qPCR analysis.

Gene	Forward	Reverse	Ref./NCBI accession number
GAPDH	ATGGGGAAGGTGAAGGTCG	TAAAAGCAGCCCTGGTGACC	[62]
LPL	GAGGTACTTTTCAGCCAGGATGTAAC	AGCTGGTCCACATCTCCAAGTC	[23,63,64]
Alk Phos	GGGAACGAGGTCACCTCCAT	TGGTCACAATGCCCACAGAT	[65]
Calponin	Ready-made as a QuantiTect Primer Assay (CNN1) (Qiagen)		[15,66,67]
TGF-β_1	TGCGGCAGCTGTACATTGA	TGGTTGTACAGGGCCAGGA	[68]
TGFBR1	CAACTCAGTCAACAGGAAGGCA	AAAGATGATCTCCAGCACAGCA	NM_004612.2
Col1A1	CCTGCGTGTACCCCACTCA	ACCAGACATGCCTCTTGTCCTT	[69]
Col4A1	GCCGTGGGACCTGCAATTACT	CGTAGGCTTCTTGAACATCT	NM_001845
LAMA4	AGTGCCATGTGCCCGAGATA	AAGAAGTAACTGGCAGCC	NM_001105206.1
N-Cad	ACCAGCCTCCAACTGGTATC	GCATGTGCCCTCAAATGAAAC	[70]

GAPDH = glyceraldehyde 3-phosphate dehydrogenase, TGF-β_1 = transforming growth factor beta 1, TGFBR1 = transforming growth factor beta receptor 1, Col1A1 = collagen type I, alpha 1, Col4A1 = collagen type IV, alpha 1, LAMA4 = laminin alpha 4 chain, N-Cad = N-Cadherin.

cycles. Results for qPCR were analysed using the $2^{-\Delta Ct}$ method to normalise gene expression to the reference gene GAPDH.

2.3.2.3. Alkaline phosphatase and lipid droplet staining. To stain for alkaline phosphatase, a solution of 1 mg/mL Fast Blue BB Salt (Sigma) and 0.2 mg/mL Naphthol AS-MX phosphate disodium salt (Sigma) (1 mg dissolved in 50 μL N-N-dimethylformamide) was prepared in 0.1 M Tris–HCl pH 9.2. Cells were washed with PBS and incubated in the prepared solution for 10 min at room temperature before washing with milli-Q water. Cells were subsequently fixed in 4% paraformaldehyde at room temperature for 20 min, washed in PBS and stained for lipid droplet accumulation using 0.5% Oil red O in isopropanol diluted 6:4 in PBS. After 30 min staining, cells were washed with PBS and images were obtained using an Olympus IX51 inverted microscope.

2.4. Rac activity inhibition analysis

Levels of N-Cad and calponin were analysed in hMSCs seeded on HCHs and LCHs in myogenic and basal medium in the presence of 25 μM Rac inhibitor, N^6-[2-[[4-(Diethylamino)-1-methylbutyl]amino]-6-methyl-4-pyrimidinyl]-2-methyl-4,6-quinolinediamine trihydrochloriden (NSC23766) (Tocris). In all cases, cells were seeded and allowed to attach to the hydrogels in standard GM for 24 h before medium was exchanged for myogenic or basal medium with or without inhibitor. NSC23766 was initially introduced after 24 h and reapplied with a medium change after 4 days.

2.5. Motility analysis

hMSCs were seeded on HCHs and LCHs at 2000 cells/cm^2 in standard growth medium. After 4 h incubation at 37 °C and 5% CO_2, images were obtained on a real-time microscope (Olympus IX81) stage with a cell culture chamber (37 °C and 5% CO_2) where cell motility time-lapse images were taken at 10 min intervals for 20 h at 10× magnification. Thereafter cell images were taken at 90 s intervals for 1.5 h at 20× magnification to determine protrusion rates (extensions and retractions). Cell velocities and protrusion rates were measured by tracking the time-lapse images using ImageJ 1.42q software (National Institute of Health, Bethesda, MD).

2.6. Immunohistochemistry

Cultures were fixed in 4% paraformaldehyde at 25 °C for 20 min, permeabilised using 0.1 wt% Trition X-100 for 5 min, blocked in 3% albumin from bovine serum (BSA)/PBS and incubated with either 1:150 anti-Tiam1 (C-16, Santa Cruz Biotechnology), 1:50 anti-Collagen-I (CL50IIIAP), 1:100 anti-collagen-IV (CP20L) or 1:250 anti-Laminin (L9393). After thorough washing the samples were incubated with 1:200 anti-mouse IgG-Alexa Fluor 488 secondary antibody (Invitrogen), 1:50 Texas Red-X phalloidin (Invitrogen) and 1:1000 Hoechst (Invitrogen) in 3% BSA/PBS for 45 min at room temperature. High resolution images were obtained using an LSR710 confocal microscope (Zeiss).

2.7. Rac biosensor analysis

2.7.1. Cell transfection

Mouse mesenchymal-derived CH3T101/2 cells are a consistently utilised cell line for studies investigating the role of mechanotransduction pathways in mesenchymal stem or progenitor cell adhesion and differentiation [25–28]. We thus chose to utilise this cell line for the development of our Rac biosensor. CH3T101/2 cells (obtained from the ATCC) were cultured in high-glucose DMEM supplemented with 10% FBS and transfected with a previously designed plasmid vector [29] when they reached 70% confluency using Lipofecatamine LTX with Plus Reagent (Life Technologies). Medium was initially exchanged with 0.5 mL of fresh growth medium per well in a 6 well tissue culture plate (TCP). For each well to be transfected, 4 μL of Lipofectamine LTX was added to 46 μL of Opti-MEM reduced serum medium while 4 μL of Plus Reagent and 1 μg of DNA were added to a separate 46 μL of Optim-MEM. After 20 min incubation at room temperature, the Lipofectamine LTX and Plus solutions were mixed and added drop-wise to the well. Cells were incubated at 37 °C and the medium was exchanged with fresh growth medium after 6 h. After stabilising for 2 days, cells were seeded onto gels in basal medium for analysis of Rac1 activation.

2.7.2. FRET microscopy

Cells were imaged live at 37 °C by confocal microscopy and images were acquired on a LSM710 Zeiss confocal microscope equipped with a 40× water immersion objective (Zeiss, Jena, GER). Donor (D) and FRET (F) channels were recorded using a 458 nm laser line and collecting the emissions in the donor (BP 470–490 nm) and acceptor (BP 530–590 nm) emission regions, respectively. In addition, crosstalk (X) and acceptor (A) channels were recorded using the 514 nm laser line for excitation and collecting the emission in the donor and acceptor emission regions. Images were acquired by sequential acquisition. For FRET measurements, a modified version of the FRET emission ratio was used to calculate this parameter on a pixel-by-pixel basis, as we described previously [30]. The FRET index was calculated for every image as the average [FRET/Donor] emission ratio for pixels located in the selected regions of interest (ROIs) in cells. FRET values were calculated for the cytosolic regions of cells and normalised to the value corresponding to the average FRET emission ratio value observed in similar regions in cells plated on LCHs. Data presented are mean FRET emission ratios calculated across the different images and their standard errors and statistical significance assessed by *t*-test.

3. Results and discussion

3.1. Proteins associated with SMC differentiation

3.1.1. TGF-β_1 and TGF-β receptor I

Chosen for its tuneable mechanical properties, PAM was used to produce high creep hydrogels (HCHs) and low creep hydrogels (LCHs) that were identical to those used in Cameron et al. [20]. They display a constant storage modulus (G′) of ~4.7 kPa but varying loss moduli (G″) of 130 Pa (HCH) and 1 Pa (LCH) respectively, at a testing frequency equivalent to that used by cells when probing a substrate [20]. Under a load representative of cell traction, the rate of creep of the LM130Pa hydrogel was shown to be more than two orders of magnitude greater than the LM1Pa hydrogel.

Substrate mechanical properties, such as stiffness, have been shown to induce secretion of cellular proteins [31], suggested to be due to the activation of mechanotransductive signalling molecules, such as Rho family GTPases. For example, constitutive activation of RhoA (a G-protein known to be affected by substrate rigidity [32]) in trabecular meshwork cells, increased their synthesis of ECM proteins [33]. Constitutive activation of Rac1, another member of the Rho family GTPases, has also been shown to increase expression of type I collagen in dermal fibroblasts [34]. Given the observed induction of SMC differentiation on HCHs [20], it is reasonable to suggest that substrate creep may also perturb mechanotransductive signalling pathways to affect the secretion of soluble or insoluble proteins involved in enhancing the differentiation potential of hMSCs. Further, the observed increase in SMC differentiation of hMSCs on substrates of increasing creep was previously

observed to be more pronounced in myogenic medium than basal medium [20]. This outcome suggested a role for soluble inductive factors in enhancing the effect of substrate creep on SMC differentiation. Given the known potential for TGF-β_1 to enhance SMC differentiation [12–15], we thus measured the expression levels of both TGF-β_1 and its receptor (TGFBR1) on these HCHs and LCHs.

When cultured in basal medium, there were no statistical differences in the expression of TGF-β_1 and TGFBR1 in hMSCs on either HCHs or LCHs after 7 days (Fig. 1A–B). This was in contrast to hMSCs cultured in myogenic medium, which showed a statistically significant increase in expression of both genes on the HCHs (Fig. 1C–D). The increased TGFBR1 expression in hMSCs on the HCHs in myogenic medium (Fig. 1D) was somewhat surprising however, as unlike TGF-β_1, no difference in TGFBR1 was seen between hMSCs in myogenic or basal media on TCP (Supplementary Fig. 1). These data suggest that increasing substrate creep may enhance SMC differentiation of hMSCs, in part, by increasing the expression of endogenous TGF-β_1 and prolonging the increase in expression of TGFBR1 upon exposure to exogenous TGF-β_1, thereby enhancing its effects.

3.1.2. Basement membrane ECM components

ECM composition is also known to be an important factor in myogenic differentiation [16,35] and due to the observed changes in TGF-β_1 expression, the effect of substrate creep on the expression of ECM proteins in hMSCs was investigated.

We first showed that transcription of COL4A1 and COL1A1 was significantly increased when hMSCs underwent SMC differentiation on TCP (Supplementary Fig. 2A–B). While LAMA4 was reduced under the same myogenic inductive conditions (Supplementary Fig. 2C), its presence in all vascular basement membranes of foetal and adult tissue [36] warranted further analysis under the influence of substrate creep. Therefore, we investigated the expression of laminin (LAMA4), type IV collagen (COL4A1) and type I collagen (COL1A1) in hMSCs on HCHs and LCHs.

hMSCs on HCHs showed statistically significant increases in the expression of COL1A1 and COL4A1 but not LAMA4 in basal medium, and a statistically significant increase in the expression of all three ECM proteins in myogenic medium (charts in Fig. 2). These increases in gene transcription were supported by qualitative increases in protein secretion (images in Fig. 2). Interestingly, the regulation of LAMA4 differed depending on whether myogenesis was induced by myogenic medium alone (when hMSCs were cultured on TCP) or by the combination of myogenic medium and substrate creep (when hMSCs were cultured on HCHs). In myogenic medium, LAMA4 expression was significantly up-regulated in hMSCs on HCHs compared to LCHs. On TCP, however, LAMA4 expression was down-regulated in myogenic medium (Supplementary Fig. 2C), which is surprising considering the core role it plays in microvessel growth [37].

Unlike collagens, little data has been reported on the effect of TGF-β_1 on laminin expression within cells, although the results of this study suggest that laminin expression is significantly reduced by exogenous TGF-β_1 signalling. Furthermore, when soluble myogenic cues (i.e. TGF-β_1) were combined with optimised

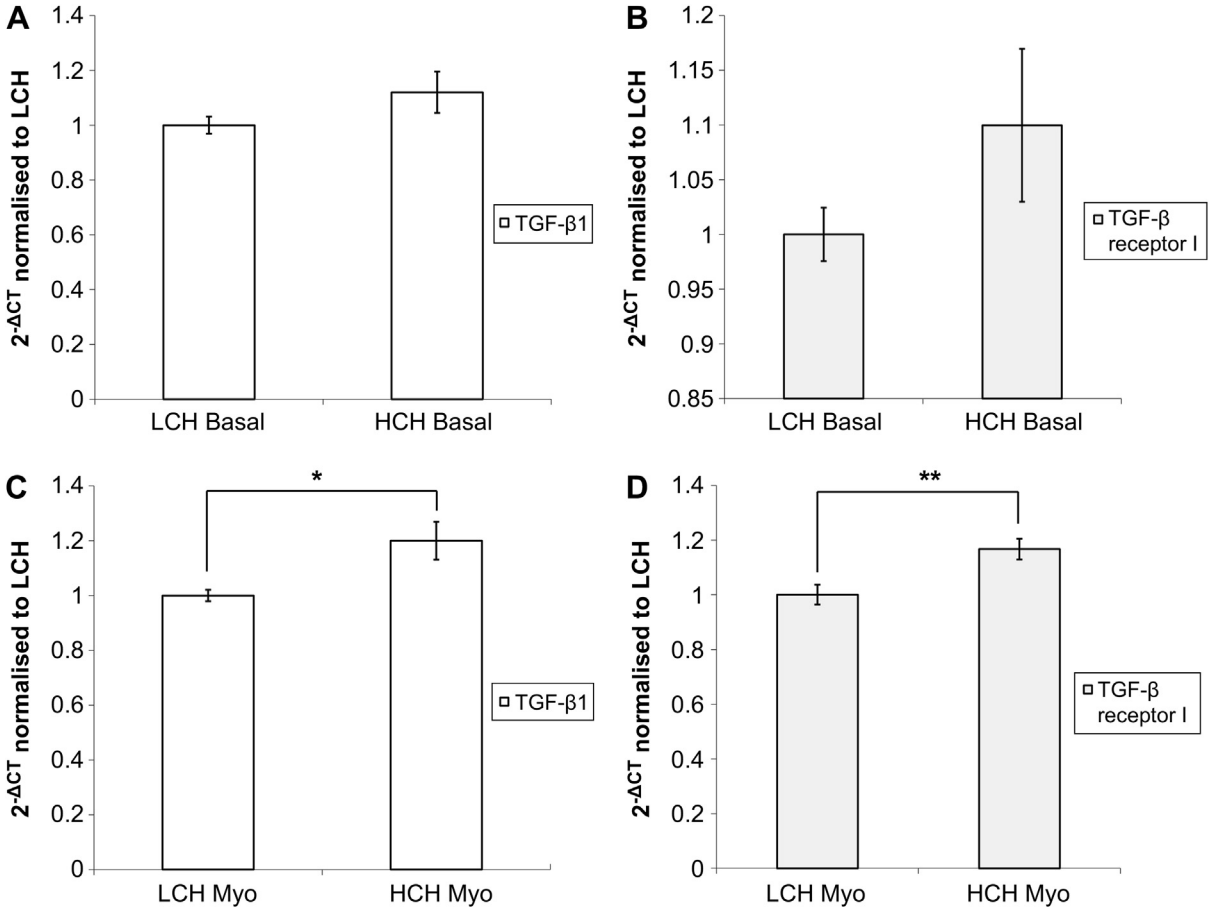

Fig. 1. Relative expression of TGF-β1 and TGFBR1 in hMSCs on substrates of different loss moduli. qRT-PCR analysis of hMSCs grown in basal medium (A–B) and myogenic induction medium (CD) on different loss modulus substrates for 7 days. Expression of TGF-β1 and TGFBR1 is relative to GAPDH and normalised to LCHs for each donor. All error bars represent ± standard error of the mean (* = $p < 0.05$, ** = $p < 0.005$).

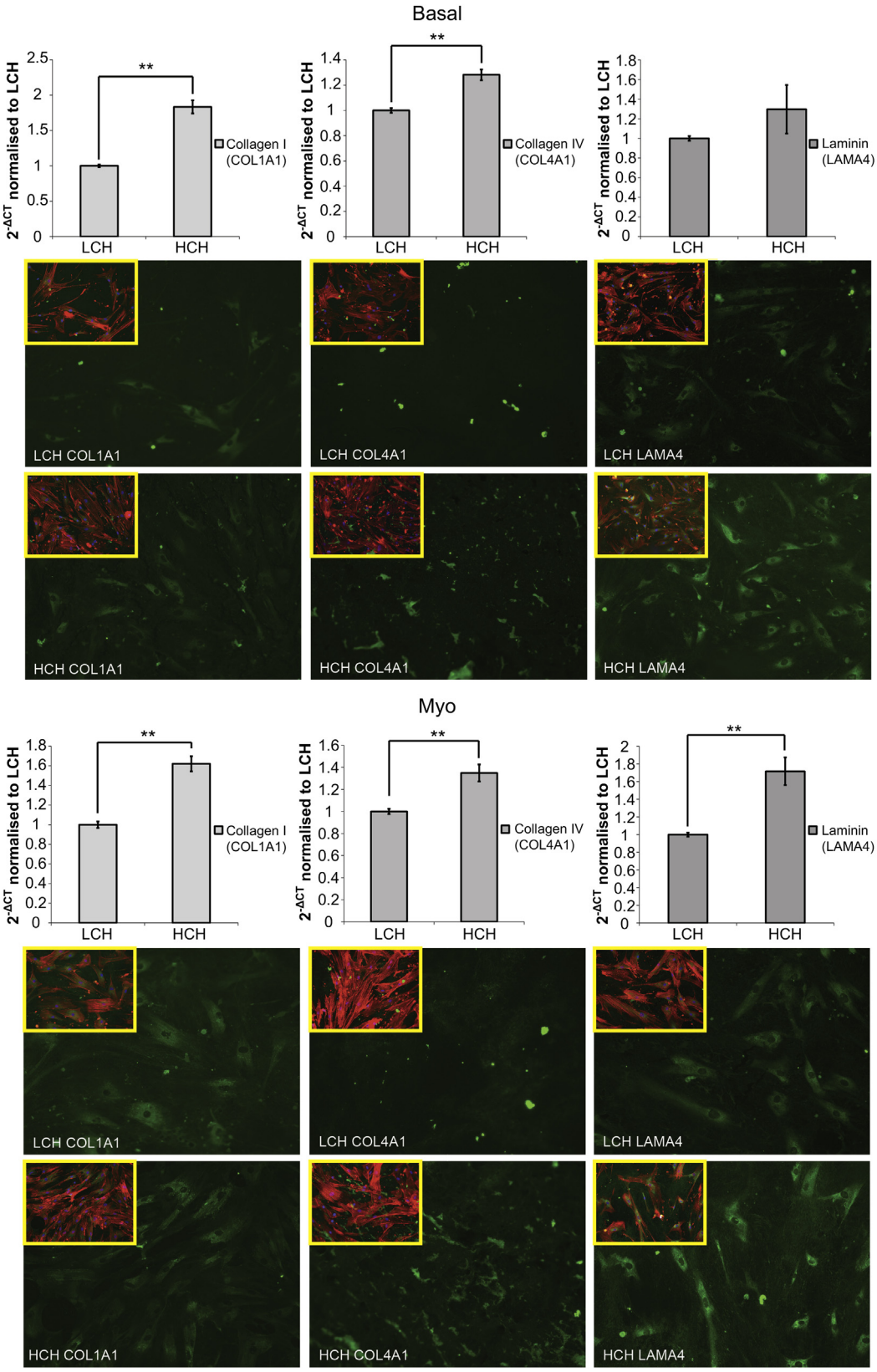

Fig. 2. Relative expression of extracellular matrix proteins in hMSCs on substrates of different loss moduli. qRT-PCR (charts) and immunohistochemistry (images) analyses of hMSCs grown in basal medium and myogenic induction medium on different loss modulus substrates for 7 days. Expression of collagen type I (COL1A1), collagen type IV (COL4A1) and laminin (LAMA4) in qPCR analysis is relative to GAPDH and normalised to LCHs for each donor. All error bars represent ± standard error of the mean (* = $p < 0.05$, ** = $p < 0.005$). Immunohistochemistry images show ECM protein (green). Insets show ECM proteins (green), nucleus (blue) and actin (red). (For interpretation of the references to colour in this figure legend, the reader is referred to the web version of this article.)

mechanical myogenic cues (i.e. increased substrate creep), laminin expression increased, thereby increasing the potential for maintenance of the differentiated SMC phenotype [38]. This is in contrast to the provision of soluble myogenic cues without optimisation of mechanical properties (i.e. on TCP), which reduced the expression of laminin (a process that occurs during the development of atherosclerotic lesions [39]). These results suggest that the differentiation and maintenance of mature SMCs may require the appropriate delivery of both soluble and mechanical cues.

3.2. Cell adhesion proteins

3.2.1. N-Cad

In addition to enhancing the expression of soluble and ECM proteins, substrate creep may also enhance SMC differentiation through its effect on proteins relating to cell–cell contact. In a study by Gao et al. [24], increased cell density was shown to enhance SMC differentiation of hMSCs via the up-regulation of the cell adhesion molecule, N-Cadherin (N-Cad). Previously, we have shown that increasing substrate creep not only increases hMSC spread area, but also proliferation [20]. This increased proliferation will inevitably lead to higher cell densities and as a result, increased cell–cell interactions. Therefore, we hypothesised that the increased cell spread area and proliferation (relating to density) of hMSCs on the HCHs could lead to increased N-Cad expression, which could then provide a mechanism for enhanced SMC differentiation.

After 7 days culture, hMSCs on HCHs showed a statistically significant increase in N-Cad expression compared to those on LCHs, in both basal and myogenic medium (Fig. 3A–B). Again, this was in line with the observed behaviour of hMSCs undergoing SMC differentiation, as exemplified by the increased expression of N-Cad when hMSCs undergo myogenic differentiation on TCP (Supplementary Fig. 3A). Whilst we have previously proposed that increased cell spread area on HCHs helps to regain the cytoskeletal tension lost as a result of substrate creep [20], cell–cell contacts may also provide a means of regaining some of this lost tension, as the forces exerted at cell–cell contacts are similar to those transduced through FAs [40]. The additional role that N-Cad plays in facilitating SMC differentiation of hMSCs suggests that this may be another mechanism that contributes to the enhanced SMC differentiation on HCHs.

3.2.2. Rac1-mediated N-Cad expression

N-Cad expression is closely related to the activity of Rac1, a member of the Rho GTPase family [41]. Over-expression of Rac1 increases N-Cad expression in hMSCs [42] while Rac1 inhibition (using an inhibitor of Rac1 activation (NSC23766)) decreased N-Cad expression on TCP, in both basal and myogenic medium (Supplementary Fig. 3B–C). We therefore hypothesised that increased N-Cad expression on HCHs may be mediated by Rac1 activity. To examine this hypothesis, the relationship between N-Cad expression and Rac1 activity on the different gels was tested.

In basal medium, hMSCs treated with 25 μM NSC23766 showed a statistically significant decrease in N-Cad expression on HCHs (Fig. 3D) but not on LCHs (Fig. 3C). This indicated that N-Cad expression was dependent on Rac1 activity on HCHs, but not on LCHs. A reversal of this behaviour was seen in myogenic medium, whereby there was a statistically significant decrease in N-Cad expression in NSC23766-treated hMSCs on LCHs (Fig. 3E) but no statistically significant effect of the treatment on N-Cad expression on the HCHs (Fig. 3F). Rac1 activity is known to be up-regulated by TGF-β-based myogenic medium [24], and therefore the increased Rac1 activity in hMSCs on LCHs in myogenic medium compared to basal medium may make them more susceptible to the effects of NSC23766 in decreasing N-Cad expression. As mentioned earlier, an increase in N-Cad expression in hMSCs on HCHs compared to those on LCHs may be a means of compensating for a loss in passive tension due to creep [20]. This data would suggest an additive effect of substrate creep and TGF-β_1 on the induction of N-Cad, which would result in a reduced impact of NSC23766 on cells on HCHs in myogenic medium.

3.3. Rac1 activity

Activated mechanotransductive signalling molecules, such as Rac1, may themselves provide a mechanism for the influence of substrate creep on SMC differentiation of hMSCs [24]. It should be noted that inhibition of Rac1 activity reduced hMSC expression of the SMC marker, calponin, irrespective of the substrate or medium (Supplementary Fig. 4). This highlights the importance of Rac1 activity to SMC differentiation of hMSCs.

A Rac FRET biosensor [29] measuring Rac1 activation was transfected within CH3T101/2 cells (a (murine) mesenchymal stem cell line commonly utilised to study the roles of mechanotransduction pathways in mesenchymal cell adhesion and differentiation [25–28]), validated and thereafter utilised to explicitly verify the hypothesis that Rac1 activity is increased with increasing substrate creep. The ability of the Rac FRET biosensor to measure variations in Rac1 activity was verified in cells expressing wild type (WT), constitutively inactivated (N17) and activated (G12V) Rac biosensor mutants (Supplementary Figs. 5 and 6). Images of cells expressing WT Rac1 biosensor were captured at 4 h (Fig. 4A–D) and 24 h (Fig. 4E–H) time points and the ratios of FRET and donor (CFP) emissions were analysed (Fig. 4B, D, F and H) to measure the respective Rac1 activities. As hypothesised, in the absence of any soluble cues, statistically significant increases in Rac1 activity were observed on the HCHs, at both 4 h and 24 h time points (Fig. 4I–J).

Unlike previous studies that have demonstrated the effect of increasing substrate stiffness on up-regulating Rho activity [32,43–46], there are divergent accounts of the effect of substrate stiffness on Rac activity. Some studies report that Rac activity increases with increasing substrate stiffness [47,48], others report that there is no effect of substrate stiffness on Rac activity [45], while it has even been suggested that Rac activity is reduced with matrix stiffness [49]. This current study clearly demonstrates the influence of time dependent deformation, or creep, a characteristic of all of viscoelastic substrates, on Rac1 activity.

The increase in Rac1 activity on HCHs fits with our previously proposed hypothesis that a reduction in passive and isometric cytoskeletal tension (a consequence of substrate creep) is compensated by an increase in isotonic tension [20]. Isotonic tension is regulated through lamellipodial protrusions, which necessitates the activation of Rac1 [50]. Interestingly, images in Fig. 4B, D, F and H suggest a higher activation of Rac1 on the periphery of cells on HCHs, supporting Rac1 activation as the driver for sustained lamellipodial activity under these substrate imposed conditions.

Given the substantial role that Rac1 plays in mediating SMC differentiation of hMSCs [24] (Supplementary Fig. 4), the increased Rac1 activity on HCHs could certainly be considered a valid mechanism contributing to the enhanced SMC differentiation on these substrates. Furthermore, a creep-induced increase in Rac1 activity has the potential to impact upon a host of other cell behaviours including motility, attachment, mitosis and cell cycle [47,51,52].

3.4. Motility and protrusion rates

As mentioned, a potential role for the increased Rac1 activity in hMSCs on HCHs is in facilitating the extension of the cell's leading edge by regulating the polymerisation of actin within lamellipodia

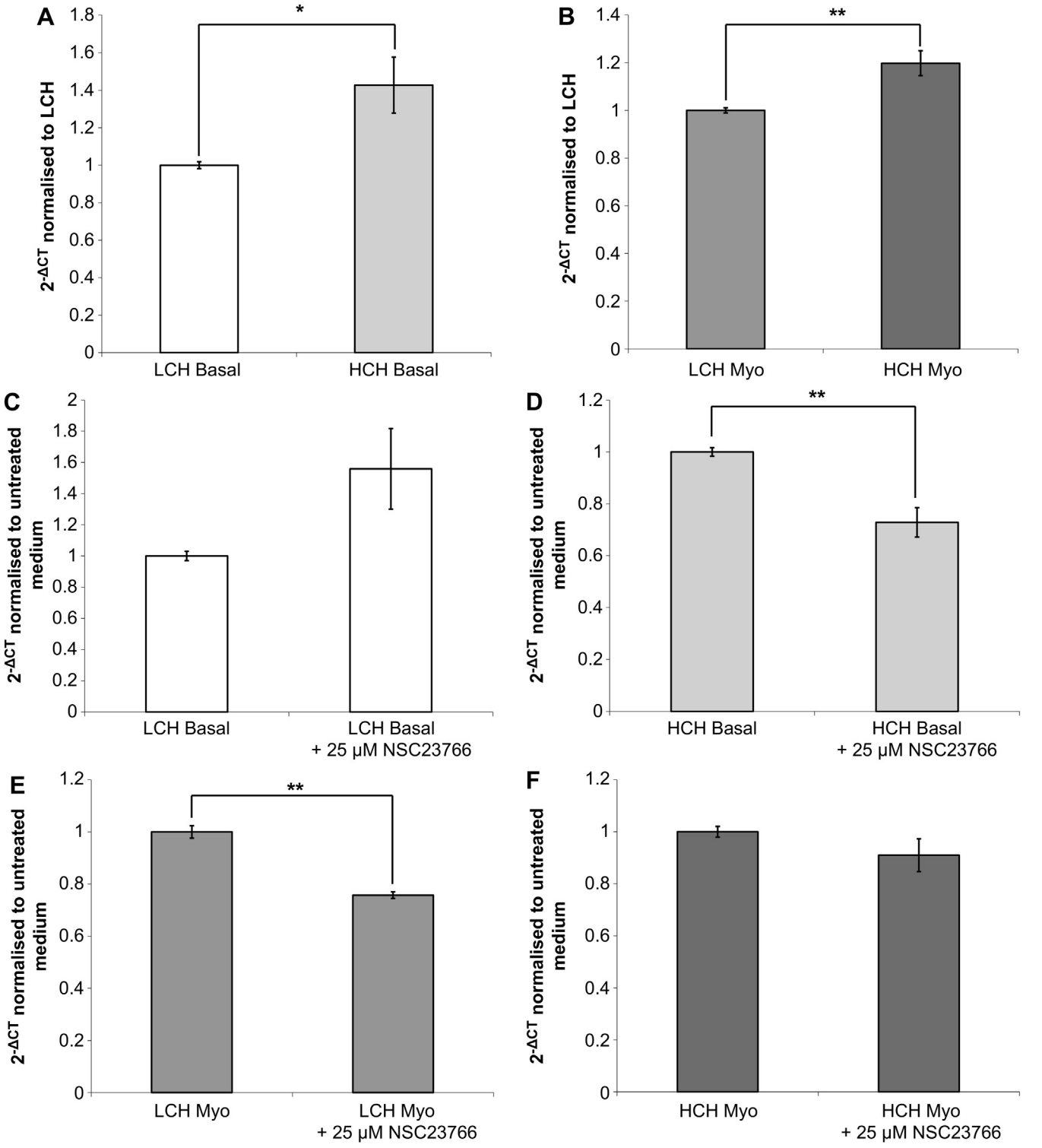

Fig. 3. N-Cad expression in hMSCs influenced by substrate loss modulus, media and Rac1 inhibition. (A and B) qRT-PCR analysis of N-Cad expression, relative to GAPDH, in hMSCs on different loss moduli substrates in basal (A) and myogenic (B) media after 7 days culture. Expression levels are normalised to LCHs for each donor. (C–F) qRT-PCR analysis of N-Cad expression in 1 untreated and Rac1 inhibited (+25 μM NSC23766) hMSCs, relative to GAPDH, when cultured LCHs (C and E) or HCHs (D and F) in basal (C and D) or myogenic (E and F) medium for 7 days. Expression levels are normalised to untreated hMSCs for each donor. All error bars represent ± standard error of the mean (* = $p < 0.05$, ** = $p < 0.005$).

[50]. To test if this is indeed the case in our system, hMSC motility and protrusion rates were analysed on HCHs and LCHs in basal medium. We found that hMSCs on HCHs showed statistically significant higher motility compared to hMSCs on LCHs (Fig. 5A and Supplementary Movies 1–2). Further, they showed a statistically significant increased rate of extension and retraction of lamellipodial protrusions (Fig. 5B and Supplementary Movies 3–4) on HCHs compared to LCHs.

Supplementary videos related to this article can be found at doi:10.1016.j.qdypi.2009.12.006

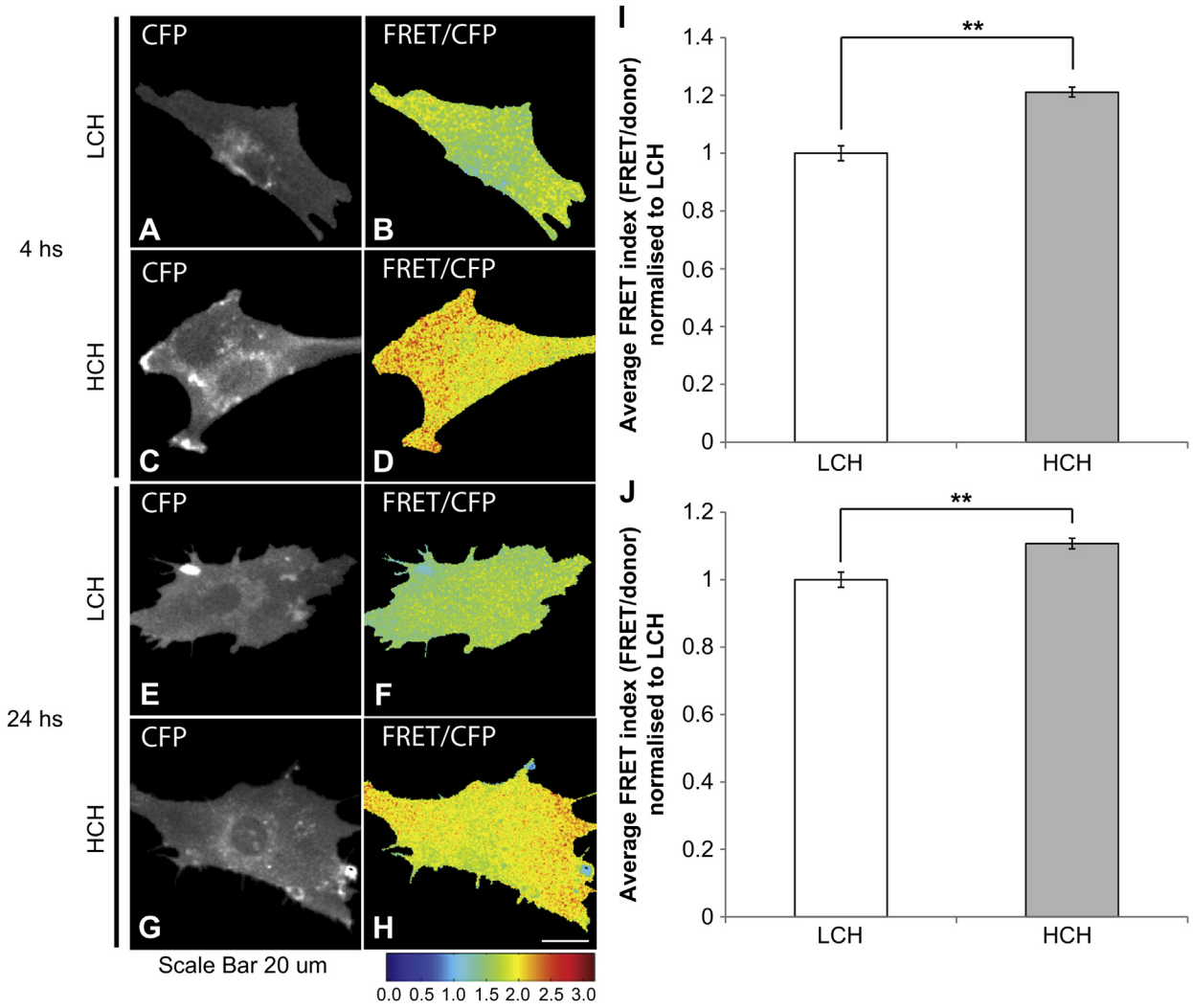

Fig. 4. FRET analysis of Rac1 biosensor transfected CH3T101/2 cells on different loss moduli substrates. (A–H) Confocal images of CH3T101/2 cells transfected with a wild type (WT) Rac1 biosensor on LCHs (A,B,E,F) and HCHs (C,D,G,H) at 4 h (A–D) and 24 h (E–H) time points. E) Average FRET index (represented in images B,D, F and H), calculated as a ratio of FRET to donor (CFP) emission, for WT transfected CH3T101/2 cells on LCHs and HCHs at 4 h (I) and 24 h (J) time points. Data was normalised to WT transfected CH3T101/2 cells on LCHs. All error bars represent ± standard error of the mean (** = $p < 0.005$).

Whilst these observations have not been reported previously, a previous study by Murrell et al. [53] has reported increased motion of epithelial cell sheets on viscous substrates, an outcome that obviously has some resonance with our results. Cells are known to move along a gradient of substrate stiffness from low compressive modulus to high compressive modulus, a phenomenon known as durotaxis [54]. It is thought that this guided movement is a result of increased tractional forces and decreased

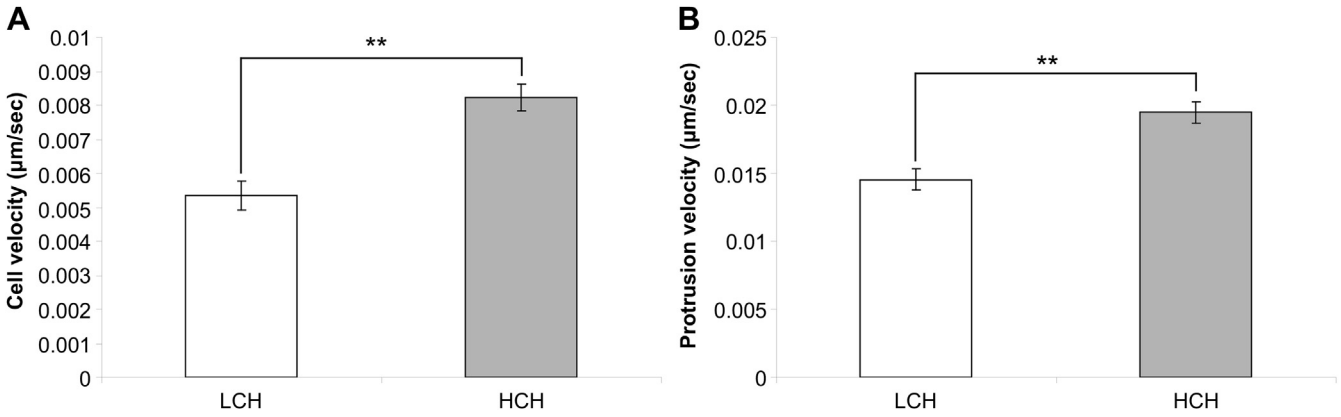

Fig. 5. Motility and protrusion rates of hMSCs on different loss moduli substrates in basal medium. (A) Motility of hMSCs on HCHs and LCHs 4 h after seeding (cell displacement measured at 10 min intervals for 20 h). (B) Extension and retraction rates of hMSC protrusions 24 h after seeding (protrusion displacement measured at 90 s intervals for 2 h). All error bars represent ± standard error of the mean (** = $p < 0.005$).

substrate (elastic) displacement (for equivalent energy inputs) on regions of increased substrate rigidity, creating a bias in the movement direction and speed respectively. On these rigid regions they are able to increase cytoskeletal tension, causing their FAs to mature and they become less motile [19,55]. We thus hypothesise that the tractional forces applied by hMSCs on both HCHs and LCHs will initially be equivalent, due to the equivalent storage (elastic) moduli of these substrates. However, due to the time-dependent dissipation of energy in HCHs, there will be a limit to the force that cells are able to exert at their FAs on these

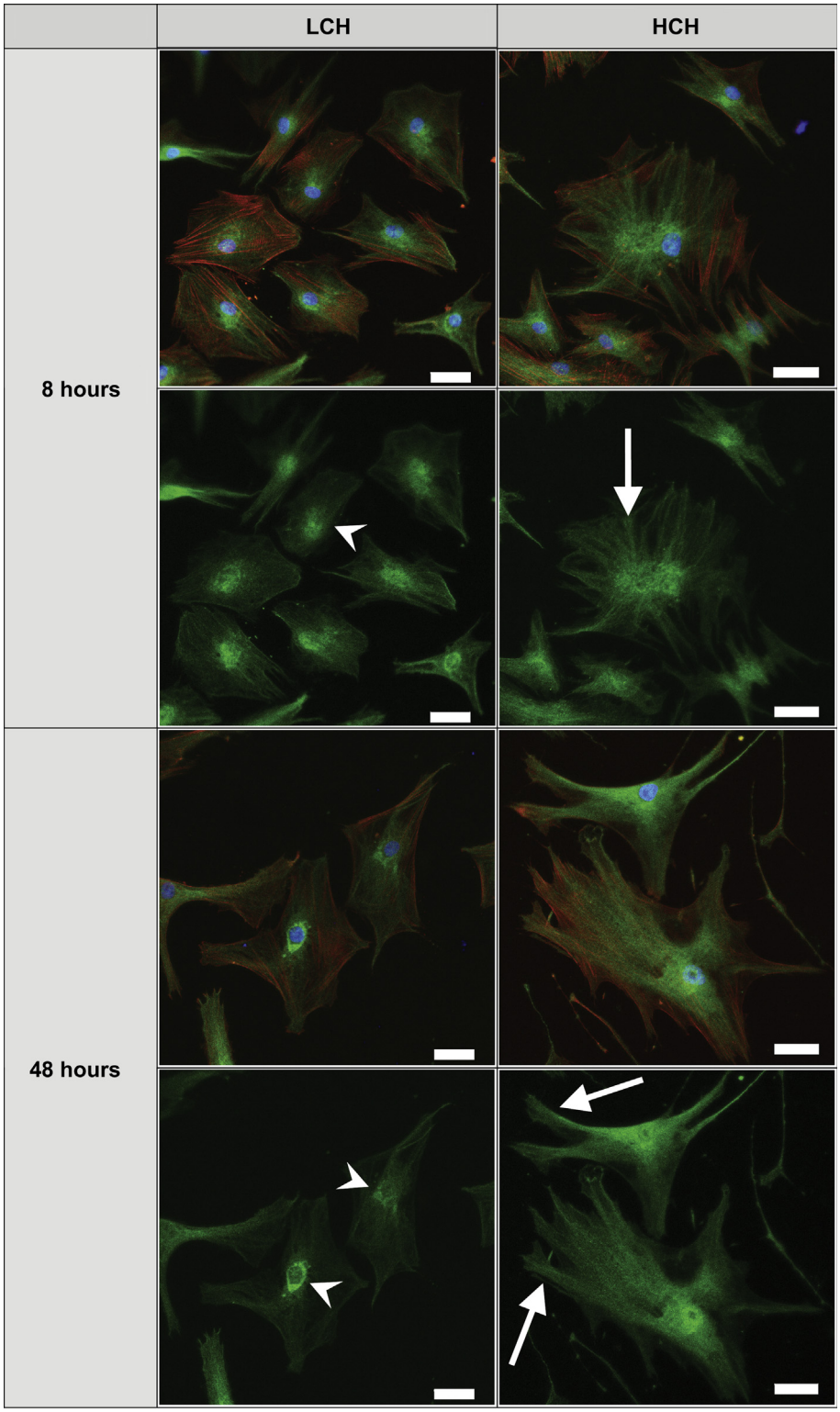

Fig. 6. Tiam1 localisation and translocation in hMSCs on different loss moduli substrates. hMSCs on LCHs and HCHs showing actin (red), nucleus (blue) and Tiam1 (green) after 8 and 48 h culture. Arrow heads indicate Tiam1 localised to the nucleus while arrows indicate translocation of Tiam1 to the cell periphery. Scale bars represent 50 μm. (For interpretation of the references to colour in this figure legend, the reader is referred to the web version of this article.)

substrates. This not only leads to smaller FAs, as confirmed by our earlier study [20], but also differing dynamics at this leading edge. Unlike LCHs, which provide a constant resistance at established FAs, the dynamic creep of HCHs will continually cause an imbalance of forces towards the leading edge where tractional forces are applied, which will then drive increased cell motility. Although there may be a depletion of tractional forces at the leading edges of hMSCs on HCHs due to substrate creep, this can be compensated for by an increase in protrusion rates, as observed on these gels (Fig. 5B), which increases the transience of FAs and avoids further time-dependent dissipation of energy at sites of adhesion. The increased hMSC motility on HCHs, with regards to both the migration and protrusion rates, suggests an increase in lamellipodia formation [56] that is likely to be mediated by the observed increase in Rac1 activation on these substrates [50].

Furthermore, the results from the current study, taken together with results from previous studies, begin to portray a cohesive story about the influence of substrate mechanical properties on the activity of Rho GTPases. Wozniak et al. [32] showed that decreasing the ability of cells to generate isometric tension, either by reducing the rigidity of their surrounding matrix or by untethering the surrounding matrix from a fixed support, increased isotonic contractility and down-regulated Rho activity. Conversely, Katsumi et al. [57] showed that increasing the cell's ability to generate isometric tension by increasing the tension in the underlying substrate down-regulated Rac activity, however this Rac activity was again up-regulated via the use of inhibitors that block myosin phosphorylation, and thus isometric contractility. We thus propose that impeding the ability of cells to generate isometric tension, via increased substrate viscous properties (creep), will lead to up-regulation of the activity of Rac. This will not only increase the ability of the cell to generate tension via isotonic mechanisms (i.e. lamellipodial protrusions), but may also down-regulate the activity of Rho, as per previous studies that have shown the down-regulation of Rho by Rac [58,59]. Therefore, given the previously demonstrated effect of stiffness on Rho activity [32,43–46], stiffness and creep properties of a material may have completely contrasting influences on Rho by up- and down-regulating its activation respectively.

A potential mediator in the up-regulation of Rac, subsequent to the creep-induced reduction of isometric tension and consequent down-regulation of Rho, is the guanine exchange factor, Tiam1. Tang et al. [60] have recently shown that inhibition of ROCK1, responsible for contributing to actin stability during cell contractility, leads to a Tiam1-mediated down-regulation of RhoA and up-regulation of Rac1. Interestingly, immunostaining of Tiam1 in the current study showed that unlike the perinuclear localisation of Tiam1 expression in hMSCs on LCHs, the localisation of Tiam1 in hMSCs on HCHs was diffuse throughout the cytosol and observed preferentially on the cell periphery, where it is necessary for the induction of Rac-mediated membrane ruffles [61] (Fig. 6). Considering the observations made by Tang et al. [60], this result provides preliminary insight into the possible upstream mechanism for the influence of substrate creep on Rac1 activation.

4. Conclusion

Enhanced protein secretion characteristic of SMC differentiation was confirmed in hMSCs adhered to viscoelastic hydrogel substrates that display increasing time-dependent deformation or creep, corroborating our previously demonstrated increase in SMC gene expression with increasing substrate creep. The mechanisms responsible for this directed differentiation were explored, using standard molecular biology techniques and a real-time Rac-1 biosensor, with the results suggesting that this effect is mediated by changes in a number of signalling pathways associated with both soluble (factor) and extracellular matrix protein production and secretion. We provide evidence that Rac1 activity is upregulated by increasing levels of substrate creep and that this is the likely driver for the enhanced expression of SMC genes in, and secretion of ECM proteins by, hMSCs on these substrates. The observed increases in rates of protrusion formation and cell migration of hMSCs on substrates with high levels of creep also align with the observed increased Rac1 activity. This work thus provides valuable insight into the effects of distinct mechanical cues, relating to separable viscous and elastic biomaterial properties, on key regulatory signalling mechanisms relevant to tissue development and stem cell fate choice. Further, as all tissues and their extracellular matrices are intrinsically viscoelastic, elucidating the effect of material creep on the behaviour and lineage commitment of hMSCs will have important implications in the development and optimisation of biomaterials for tissue engineering applications.

Disclosure of potential conflicts of interest

The authors declare no competing financial interests of potential conflicts of interest.

Acknowledgements

We gratefully acknowledge Dr Erik Miller for discussions on polyacrylamide mechanical testing and Dr Gary Brooke from the Mater Medical Research Institute for providing hMSCs. This study was financially supported by the Australian Research Council Discovery Grants Scheme (DP 1095429 and DP110104446), the Cooperative Research Centre for Polymers as well as the School of Chemical Engineering and the Australian Institute of Bioengineering and Nanotechnology at The University of Queensland. This work was partly performed at the Australian National Fabrication Facility, a company established under the National Collaborative Research Infrastructure Strategy to provide nano- and microfabrication facilities for Australia's researchers.

Appendix A. Supplementary data

Supplementary data related to this article can be found online at http://dx.doi.org/10.1016/j.biomaterials.2013.11.023.

References

[1] Discher DE, Janmey P, Wang Y-l. Tissue cells feel and respond to the stiffness of their substrate. Science 2005;310(5751):1139–43.
[2] Schwartz MA, Ginsberg MH. Networks and crosstalk: integrin signalling spreads. Nat Cell Biol 2002;4(4):65–8.
[3] Engler AJ, Sen S, Sweeney HL, Discher DE. Matrix elasticity directs stem cell lineage specification. Cell 2006;126(4):677–89.
[4] Winer JP, Janmey PA, McCormick ME, Funaki M. Bone marrow-derived human mesenchymal stem cells become quiescent on soft substrates but remain responsive to chemical or mechanical stimuli. Tissue Eng Part A 2009;15(1):147–54.
[5] Rowlands AS, George PA, Cooper-White JJ. Directing osteogenic and myogenic differentiation of MSCs: interplay of stiffness and adhesive ligand presentation. Am J Physiol Cell Physiol 2008;295(4):1037–44.
[6] Kundu AK, Putnam AJ. Vitronectin and collagen I differentially regulate osteogenesis in mesenchymal stem cells. Biochem Biophys Res Co 2006;347(1):347–57.
[7] Dalby MJ, Gadegaard N, Tare R, Andar A, Riehle MO, Herzyk P, et al. The control of human mesenchymal cell differentiation using nanoscale symmetry and disorder. Nat Mater 2007;6(12):997–1003.
[8] Yim EKF, Darling EM, Kulangara K, Guilak F, Leong KW. Nanotopography-induced changes in focal adhesions, cytoskeletal organization, and mechanical properties of human mesenchymal stem cells. Biomaterials 2010;31(6):1299–306.

[9] Gutierrez JA, Perr HA. Mechanical stretch modulates TGF-β1 and α1(I) collagen expression in fetal human intestinal smooth muscle cells. Am J Physiol Gastr L 1999;277(5):G1074–80.
[10] O'Callaghan CJ, Williams B. Mechanical strain-induced extracellular matrix production by human vascular smooth muscle cells: role of TGF-{beta}1. Hypertension 2000;36(3):319–24.
[11] Yasuda T, Kondo S, Homma T, Harris RC. Regulation of extracellular matrix by mechanical stress in rat glomerular mesangial cells. J Clin Inves 1996;98(9):1991–2000.
[12] Narita Y, Yamawaki A, Kagami H, Ueda M, Ueda Y. Effects of transforming growth factor-{beta}1 and ascorbic acid on differentiation of human bone-marrow-derived mesenchymal stem cells into smooth muscle cell lineage. Cell Tissue Res 2008;333(3):449–59.
[13] Kinner B, Zaleskas JM, Spector M. Regulation of smooth muscle actin expression and contraction in adult human mesenchymal stem cells. Exp Cell Res 2002;278(1):72–83.
[14] Wang D, Park JS, Chu JSF, Krakowski A, Luo K, Chen DJ, et al. Proteomic profiling of bone marrow mesenchymal stem cells upon transforming growth factor beta 1 stimulation. J Biol Chem 2004;279(42):43725–34.
[15] Au P, Tam J, Fukumura D, Jain RK. Bone marrow-derived mesenchymal stem cells facilitate engineering of long-lasting functional vasculature. Blood 2008;111(9):4551–8.
[16] Suzuki S, Narita Y, Yamawaki A, Murase Y, Satake M, Mutsuga M, et al. Effects of extracellular matrix on differentiation of human bone marrow-derived mesenchymal stem cells into smooth muscle cell lineage: utility for cardiovascular tissue engineering. Cells Tissues Organs 2010;191(4):269–80.
[17] Xiao Q, Luo Z, Pepe AE, Margariti A, Zeng L, Xu Q. Embryonic stem cell differentiation into smooth muscle cells is mediated by Nox4-produced H_2O_2. Am J Physiol Cell Physiol 2009;296(4):C711–23.
[18] Xiao Q, Wang G, Luo Z, Xu Q. The mechanism of stem cell differentiation into smooth muscle cells. Thromb Haemost 2010;104(3):440–8.
[19] Geiger B, Spatz JP, Bershadsky AD. Environmental sensing through focal adhesions. Nat Rev Mol Cell Biol 2009;10(1):21–33.
[20] Cameron AR, Frith JE, Cooper-White JJ. The influence of substrate creep on mesenchymal stem cell behaviour and phenotype. Biomaterials 2011;32(26):5979–93.
[21] Ingber DE. Cellular tensegrity: defining new rules of biological design that govern the cytoskeleton. J Cell Sci 1993;104(3):613–27.
[22] Ingber D, Tensegrity I. Cell structure and hierarchical systems biology. J Cell Sci 2003;116(7):1157–73.
[23] McBeath R, Pirone DM, Nelson CM, Bhadriraju K, Chen CS. Cell shape, cytoskeletal tension, and RhoA regulate stem cell lineage commitment. Dev Cell 2004;6(4):483–95.
[24] Gao L, McBeath R, Chen CS. Stem cell shape regulates a chondrogenic versus myogenic fate through Rac1 and N-cadherin. Stem Cells 2010;28(3):564–72.
[25] Martin I, Jakob M, Schäfer D, Dick W, Spagnoli G, Heberer M. Quantitative analysis of gene expression in human articular cartilage from normal and osteoarthritic joints. Osteoarthr Cartil 2001;9(2):112–8.
[26] Hudson JE, Mills RJ, Frith JE, Brooke G, Jaramillo-Ferrada P, Wolvetang EJ, et al. A defined media and substrate for expansion of human mesenchymal stromal cell progenitors that enriches for osteo- and chondro-genic precursors. Stem Cells Dev 2011;20(1).
[27] Frith JE, Thomson B, Genever P. Dynamic three-dimensional culture methods enhance mesenchymal stem cell properties and increase therapeutic potential. Tissue Eng Part C Methods 2009;16(4):735–49.
[28] Wang C, Lau TT, Loh WL, Su K, Wang D-A. Cytocompatibility study of a natural biomaterial crosslinker—genipin with therapeutic model cells. J Biomed Mater Res B 2011;97B(1):58–65.
[29] Miano JM, Olson EN. Expression of the smooth muscle cell calponin gene marks the early cardiac and smooth muscle cell lineages during mouse embryogenesis. J Biol Chem 1996;271(12):7095–103.
[30] Ball SG, Shuttleworth AC, Kielty CM. Direct cell contact influences bone marrow mesenchymal stem cell fate. Int J Biochem Cell Biol 2004;36(4):714–27.
[31] Tan G-K, Dinnes DLM, Myers PT, Cooper-White JJ. Effects of biomimetic surfaces and oxygen tension on redifferentiation of passaged human fibrochondrocytes in 2D and 3D cultures. Biomaterials 2011;32(24):5600–14.
[32] Dyson JA, Genever PG, Dalgarno KW, Wood DJ. Development of custom-built bone scaffolds using mesenchymal stem cells and apatite-wollastonite glass-ceramics. Tissue Eng 2007;13(12):2891–901.
[33] Ferreira MC, Witz CA, Hammes LS, Kirma N, Petraglia F, Schenken RS, et al. Activin A increases invasiveness of endometrial cells in an in vitro model of human peritoneum. Mol Hum Reprod 2008;14(5):301–7.
[34] Lee JS, Ha L, Kwon IK, Lim JY. The role of focal adhesion kinase in BMP4 induction of mesenchymal stem cell adipogenesis. Biochem Biophys Res Co 2013;435(4):696–701.
[35] Andalib MN, Lee JS, Ha L, Dzenis Y, Lim JY. The role of RhoA kinase (ROCK) in cell alignment on nanofibers. Acta Biomater 2013;9(8):7737–45.
[36] Rossol-Allison J, Stemmle LN, Swenson-Fields KI, Kelly P, Fields PE, McCall SJ, et al. Rho GTPase activity modulates Wnt3a/β-catenin signaling. Cell Sig 2009;21(11):1559–68.
[37] Arnsdorf EJ, Tummala P, Kwon RY, Jacobs CR. Mechanically induced osteogenic differentiation – the role of RhoA, ROCKII and cytoskeletal dynamics. J Cell Sci 2009;122(4):546–53.
[38] Itoh RE, Kurokawa K, Ohba Y, Yoshizaki H, Mochizuki N, Matsuda M. Activation of Rac and Cdc42 video imaged by fluorescent resonance energy transfer-based single-molecule probes in the membrane of living cells. Mol Cell Biol 2002;22(18):6582–91.
[39] Ratheesh A, Gomez GA, Priya R, Verma S, Kovacs EM, Jiang K, et al. Centralspindlin and alpha-catenin regulate Rho signalling at the epithelial zonula adherens. Nat Cell Biol 2012;14(8):818–28.
[40] Williams CM, Engler AJ, Slone RD, Galante LL, Schwarzbauer JE. Fibronectin expression modulates mammary epithelial cell proliferation during acinar differentiation. Cancer Res 2008;68(9):3185–92.
[41] Wozniak MA, Desai R, Solski PA, Der CJ, Keely PJ. ROCK-generated contractility regulates breast epithelial cell differentiation in response to the physical properties of a three-dimensional collagen matrix. J Cell Biol 2003;163(3):583–95.
[42] Pattabiraman PP, Rao PV. Mechanistic basis of Rho GTPase-induced extracellular matrix synthesis in trabecular meshwork cells. Am J Physiol Cell Physiol 2010;298(3):C749–63.
[43] Shi-wen X, Liu S, Eastwood M, Sonnylal S, Denton CP, Abraham DJ, et al. Rac inhibition reverses the phenotype of fibrotic fibroblasts. PLoS ONE 2009;4(10):e7438.
[44] Beqaj S, Jakkaraju S, Mattingly RR, Pan D, Schuger L. High RhoA activity maintains the undifferentiated mesenchymal cell phenotype, whereas RhoA down-regulation by laminin-2 induces smooth muscle myogenesis. J Cell Biol 2002;156(5):893–903.
[45] Fujiwara H, Gu J, Sekiguchi K. Rac regulates integrin-mediated endothelial cell adhesion and migration on laminin-8. Exp Cell Res 2004;292(1):67–77.
[46] Thyboll J, Kortesmaa J, Cao R, Soininen R, Wang L, Iivanainen A, et al. Deletion of the laminin {alpha}4 chain leads to impaired microvessel maturation. Mol Cell Biol 2002;22(4):1194–202.
[47] Thyberg J, Blomgren K, Roy J, Tran PK, Hedin U. Phenotypic modulation of smooth muscle cells after arterial injury is associated with changes in the distribution of laminin and fibronectin. J Histochem Cytochem 1997;45(6):837–46.
[48] Raines EW, Koyama H, Carragher NO. The extracellular matrix dynamically regulates smooth muscle cell responsiveness to PDGFa. Ann NY Acad Sci 2000;902(1):39–52.
[49] Ganz A, Lambert M, Saez A, Silberzan P, Buguin A, Mège RM, et al. Traction forces exerted through N-cadherin contacts. Biol Cell 2006;98(12):721–30.
[50] Takaishi K, Sasaki T, Kotani H, Nishioka H, Takai Y. Regulation of cell-cell adhesion by Rac and Rho small G proteins in MDCK cells. J Cell Biol 1997;139(4):1047–59.
[51] Woods A, Wang G, Dupuis H, Shao Z, Beier F. Rac1 signaling stimulates N-cadherin expression, mesenchymal condensation, and chondrogenesis. J Biol Chem 2007;282(32):23500–8.
[52] Kim TJ, Seong J, Ouyang M, Sun J, Lu S, Hong JP, et al. Substrate rigidity regulates Ca2+ oscillation via RhoA pathway in stem cells. J Cell Physiol 2009;218(2):285–93.
[53] Paszek MJ, Zahir N, Johnson KR, Lakins JN, Rozenberg GI, Gefen A, et al. Tensional homeostasis and the malignant phenotype. Cancer Cell 2005;8(3):241–54.
[54] Keung AJ, de Juan-Pardo EM, Schaffer DV, Kumar S. Rho GTPases mediate the mechanosensitive lineage commitment of neural stem cells. Stem Cells 2011;29(11):1886–97.
[55] Provenzano PP, Inman DR, Eliceiri KW, Keely PJ. Matrix density-induced mechanoregulation of breast cell phenotype, signaling and gene expression through a FAK-ERK linkage. Oncogene 2009;28(49):4326–43.
[56] Kocgozlu L, Rabineau M, Koenig G, Haikel Y, Schaaf P, Freund J-N, et al. The control of chromosome segregation during mitosis in epithelial cells by substrate elasticity. Biomaterials 2012;33(3):798–809.
[57] Kocgozlu L, Lavalle P, Koenig G, Senger B, Haikel Y, Schaaf P, et al. Selective and uncoupled role of substrate elasticity in the regulation of replication and transcription in epithelial cells. J Cell Sci 2010;123(1):29–39.
[58] Friedland JC, Lakins JN, Kazanietz MG, Chernoff J, Boettiger D, Weaver VM. α6β4 integrin activates Rac-dependent p21-activated kinase 1 to drive NF-κB-dependent resistance to apoptosis in 3D mammary acini. J Cell Sci 2007;120(20):3700–12.
[59] Nobes CD, Hall A. Rho, Rac, and Cdc42 GTPases regulate the assembly of multimolecular focal complexes associated with actin stress fibers, lamellipodia, and filopodia. Cell 1995;81(1):53–62.
[60] Yang FC, Atkinson SJ, Gu Y, Borneo JB, Roberts AW, Zheng Y, et al. Rac and Cdc42 GTPases control hematopoietic stem cell shape, adhesion, migration, and mobilization. Proc Natl Acad Sci U S A 2001;98(10):5614–8.
[61] Klein EA, Yin L, Kothapalli D, Castagnino P, Byfield FJ, Xu T, et al. Cell-cycle control by physiological matrix elasticity and in vivo tissue stiffening. Curr Biol 2009;19(18):1511–8.
[62] Murrell M, Kamm R, Matsudaira P. Substrate viscosity enhances correlation in epithelial sheet movement. Biophys J 2011;101(2):297–306.
[63] Lo C-M, Wang H-B, Dembo M, Wang Y-l. Cell movement is guided by the rigidity of the substrate. Biophys J 2000;79(1):144–52.
[64] Pelham RJ, Wang Y-l. Cell locomotion and focal adhesions are regulated by substrate flexibility. Proc Natl Acad Sci U S A 1997;94(25):13661–5.
[65] Dalby MJ, Oreffo ROC. Chapter 3: Mesenchymal stem cells and controlled nanotopography. In: Reisner DE, editor. Bionanotechnology: global prospects. Boca Raton: CRC Press; 2009. pp. 35–43.

[66] Katsumi A, Milanini J, Kiosses WB, del Pozo MA, Kaunas R, Chien S, et al. Effects of cell tension on the small GTPase Rac. J Cell Biol 2002;158(1):153–64.
[67] Nimnual AS, Taylor LJ, Bar-Sagi D. Redox-dependent downregulation of Rho by Rac. Nat Cell Biol 2003;5(3):236–41.
[68] Sander EE, ten Klooster JP, van Delft S, van der Kammen RA, Collard JG. Rac downregulates Rho activity reciprocal balance between both GTPases determines cellular morphology and migratory behavior. J Cell Biol 1999;147(5):1009–22.
[69] Tang AT, Campbell WB, Nithipatikom K. ROCK1 feedback regulation of the upstream small GTPase RhoA. Cell Sig 2012;24(7):1375–80.
[70] Michiels F, Stam JC, Hordijk PL, van der Kammen RA, Stalle LR-V, Feltkamp CA, et al. Regulated membrane localization of Tiam1, mediated by the NH_2-terminal pleckstrin homology domain, is required for Rac-dependent membrane ruffling and C-Jun NH_2-terminal kinase activation. J Cell Biol 1997;137(2):387–98.